Power System Technology
ISSN:1000-3673

Received: 06-10-2024 Revised: 15-11-2024 Accepted: 25-02-2025

Sensitivity Ehancement Analysis due to Different Coating Materials of Ultra-Weak Fibre Bragg Gratings based Depth Sensor for Underwater Applications

Gopalakrishnamurthy C R[a*], Karthik Palani[b*], Kripa K B[c*], B N Manjunatha Reddy[d*]

[a]Research Scholar, Department of Computer Science and Engineering affiliate to Visvesvaraya Technological University, K R Puram, Bengaluru-560036 India*
[b]Professor, Department of Computer Science and Engineering affiliate to Visvesvaraya Technological University, K R Purma, Bengaluru-560036 India*
[c]Research Scholar, Department of Electronics and Communication Engineering affiliate to Visvesvaraya Technological University, K R Puram, Bengaluru-560036 India*
*[d]*Professor and Associate Dean, Department of Artifical Intelligence and Machine Learning affiliate to Visvesvaraya Technological University, K R Puram, Bengaluru-560036 India*

Abstract: -Ocean depth is an important quantity for a variety of nautical applications, including surveillance and navigation. Many maritime applications, such as surveillance, navigation, and environmental monitoring, rely on accurate water depth measurements. Traditional depth-sensing devices may have limited sensitivity and accuracy, especially in harsh underwater environments. In this manuscript, sensitivity enhancement analysis because of various coating materials of ultra-weak fibre bragg gratings dependent depth sensor for underwater applications (SEACM-UWFBG-DSUA) is proposed. The SEACM-UWFBG-DSUA method presents a experiment of an ocean depth sensor depending upon Ultra-Weak Fibre Bragg Gratings (UWFBG). It illustrates the cause of applying a consistent layer of coating on sensitivity. A variety of resources, like metals as well as polymers such as aluminum (Al), silica (SiO2), indium (In), zinc (Zn), as well as a polymer, Polytetrafluoroethylene (PTFE), is evaluated for sensitivity and general practicality. Modulating the grating using chirp or apodization can increase its sensitivity. The study shows, apodized Polytetrafluoroethylene-coated gratings is best suited for applications, with a high sensitivity of 24.54 pm/m compared to existing techniques such as Sensitivity improvement examine because of diverse coating material of FBG-dependent depth sensor for underwater applications (SEA-FBG-DSUA) respectively.

Keywords: Apodization, Chirp, coating materials, optical sensors, Polytetrafluoroethylene, polymers, sensitivity;

Power System Technology
ISSN:1000-3673
Received: 06-10-2024 Revised: 15-11-2024 Accepted: 25-02-2025

1. INTRODUCTION

As scientific research into the marine environment intensifies, there is a growing need for sensors capable of detecting subtle modifies in key ocean properties include temperature, depth. The fibre-optic sensors have emerged as a major advancement in this area due to their high sensitivity, fast response, compact size, robustness, and versatility. Enhancing the sensing capabilities of traditional Single Mode Fibre (SMF) through periodic modulation of the refractive index, known as Fibre Bragg Grating (FBG) offers substantial improvements in performance. [1-3]. An innovative approach to pressure sensing utilizing a even FBG sensor integrated into a standard Single Mode Fibre, paving the way for a new application in depth sensing. Unlike conventional depth gauges that utilize a piezoelectric transducer to detect pressure changes by generating an electrical response in materials like quartz, this method offers a novel alternative [4-6]. Although this tool offers a reasonable frequency reply, its low output necessitates extensive additional circuitry. In addition, the crystal can be affected by dissolving in damp or humid environments. Alternatively, sound navigation with ranging (SONAR) technology is broadly utilized in this field. [7-9].A sound pulse is emitted to measure absolute depth by timing its return, but this method cannot gauge depth at arbitrary points in the ocean. Fibre-optic sensors, with their distinct advantages, offer a viable alternative. Recent advancements in fibre-optic pressure sensors highlight their growing relevance, particularly due to the high sensitivity of Fibre Bragg Gratings (FBGs) to strain. This sensitivity has expanded research into other mechanical parameters like force as well as pressure, lead for broader industrial applications [11–13]. FBGs have been employed to enhance the strength of polymer optical fibres, and various alternative pressure sense applications utilizing visual fibres is documented in the literature, demonstrating outstanding sensitivity [14]. Low pressure sensors have been determined to be appropriate for use in chemical and medical applications. Previous research has also used fibre-optic sensors for depth detection. The Fabry-Perot Interferometer (FPI) and FBG sensor were coupled to detect underwater temperature and depth simultaneously [15]. Accurate water depth measurement is essential for maritime activities such as surveillance, navigation, and environmental monitoring, yet traditional sensors often struggle with sensitivity and accuracy in challenging underwater environments. This research focuses on enhancing the performance of Fibre Bragg Grating (FBG) depth sensors by evaluating various coating materials, ultimately identifying PTFE as the optimal choice. Additionally, the study incorporates modulation techniques like chirp and apodization to further improve sensor effectiveness in marine settings. These advancements not only boost sensor reliability but also pave the way for innovative optical sensing applications in oceanography and marine exploration.

The main contribution of this investigation work is summarized as follows,

- In this research work, SEACM-UWFBG-DSUA method is proposed.
- The article presents a experiment of an ocean depth sensor utilizing UWFBG.

Power System Technology
ISSN:1000-3673
Received: 06-10-2024 Revised: 15-11-2024 Accepted: 25-02-2025

- A variety of diverse materials, like metals as well as polymers, such as Polymer (PMMA), Titanium Oxide (TiO2), Boron Nitride (BN), Magnesium Oxide (MgO) and PTFE are evaluated for their sensitivity efficacy with common feasibility.
- The efficiency of the proposed SEACM-UWFBG-DSUA method is compared with the help of performances like sensitivity and compared to the existing SEA-FBG-DSUA respectively.

This describes exactly the remaining manuscript is organized: The literature review is presented in Part 2, the proposed methodology is shown in Part 3, the results and discussions are shown in Part 4, and the manuscript is concluded in Part 5.

2. LITERATURE REVIEW

Several research works presented in the literatures were based on Sensitivity Enhancement Analysis for Underwater Applications; few of them were reviewed here,

In 2020, Chakravartula, V, et.al [16] have suggested the sensitivity improvement examine because of diverse coating materials of FBG-dependent depth sensor for underwater applications. It simulates an ocean depth sensor using aneven FBG, demonstrating how a consistent coating layer influences sensitivity. Various materials, such as metals and polymers, were assessed to determine their impact on sensitivity and overall feasibility. It provides high Poisson's ratio and low Photo elastic coefficient.

In 2024, Naumann, C, et.al, [17] have presented the unstable characterization of FBG temperature sensors. It presents the structure along with growth of FBG hydroacoustic pressure sensors aimed at enhancing underwater communication. The lateral hole package was modelled as well as determined using Ansys Multi-physics. To optimize performance, 3diverse coating materials titanium, polyamide, and gold were applied to the core fibre of the sensor, each imparting distinct mechanical properties to the structure. It provides higher Young's modulus (GPa) with less Poisson's ratio.

In 2024, Haque, M.A, et.al, [18] have presented the mathematical examine of metal-insulator-metal (MIM) waveguide-combined magnetic field sensor (MFS) operating on sub-wavelength measures. Using the MIM waveguide structure with a W-shaped cavity fill by magnetic fluid, it suggests a novel plasmonic MFS. The sensor leverages the unique characteristics of surface plasmonpolaritons alongside the magneto-visual characteristics of the by magnetic fluid to induce shifts in resounding wavelengths. It provides high Photo elastic coefficient and low Young's modulus (GPa).

In 2024,Macheso, P.S, et.al, [19] have presented the modelling and examine the FBG temperature sensor for IoT systems (FBG-4-IoT). It suggested a targeted design for the parameters of FBG sensors to improve their performance in temperature measurement,

Power System Technology
ISSN:1000-3673
Received: 06-10-2024 Revised: 15-11-2024 Accepted: 25-02-2025

enabling more effective integration into IoT applications. It provides high Poisson's ratio and Photo elastic coefficient.

In 2023, Liu, X, et.al, [20] have presented the high sensitivity sensor for concurrent underwater assessment of salinity as well as temperature depending upon higher birefringent asymmetric photonic crystal fibre. It presents an innovative miniature fiber sensor designed for concurrent monitoring of underwater salinity as well as temperature through simulation. A higher bi-refringent, asymmetric full-circular hole photonic crystal fibre (HB-A-FCH PCF) with a wavelength of 2.2 µm and a birefringence of 2.83 × 10^-3 is used in the sensor. It provides maximal ratio of Poisson with minimal Young's modulus (GPa).

3.Proposed Methodology

In this section, the SEACM-UWFBG-DSUA system is proposed for simulating an ocean depth sensor utilizing Ultra Weak Fibre Bragg Gratings (UWFBG) by enhancing the sensitivity.

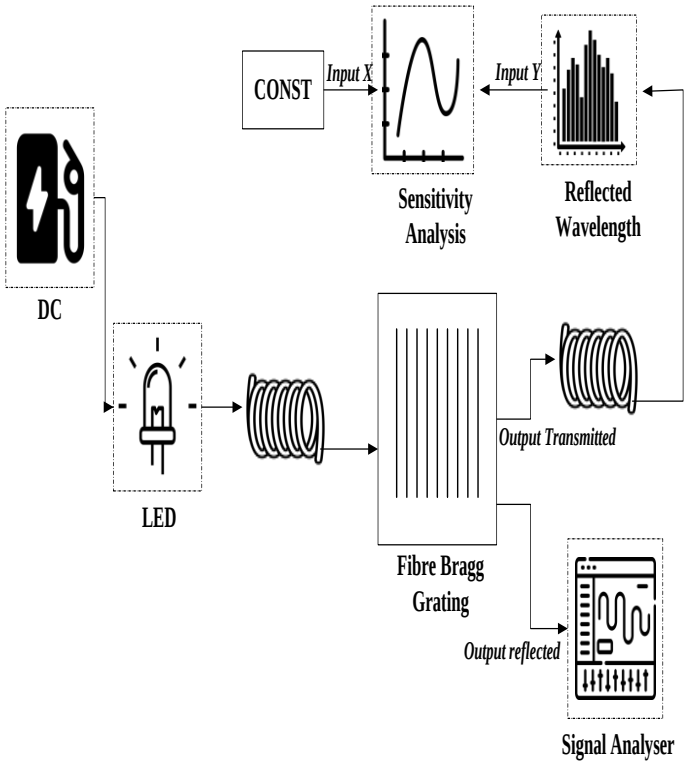

Figure 1: Block diagram of the proposed SEACM-UWFBG-DSUA

Figure 1 depicts the block diagram of SEACM-UWFBG-DSUA system. The proposed SEACM-UWFBG-DSUA investigates the effects of applying a uniform coating layer on sensor sensitivity, comparing various materials, including metals and polymers such as PMMA, TiO2, BN, MgO, and PTFE. The results reveal that PTFE achieves the maximum sensitivity on the basis of wavelength shift per unit depth modify. Further sensitive

Power System Technology
ISSN:1000-3673
Received: 06-10-2024 Revised: 15-11-2024 Accepted: 25-02-2025

improvement is achieved through grating modulations like chirp or apodization, with apodized PTFE-coated gratings demonstrating a high sensitive of 24.54 pm/m. The study emphasizes that choosing the right coating is essential for enhancing sensitivity while ensuring durability and linearity, potentially advancing the development of high sensitivity with accurate visual sensors for undersea depth measurement.

3.1 System model

The Bragg grating length of the fibre Bragg grating (FBG) sensor is 10 mm. The 3D image of FBG structure is displayed in Fig. 2.

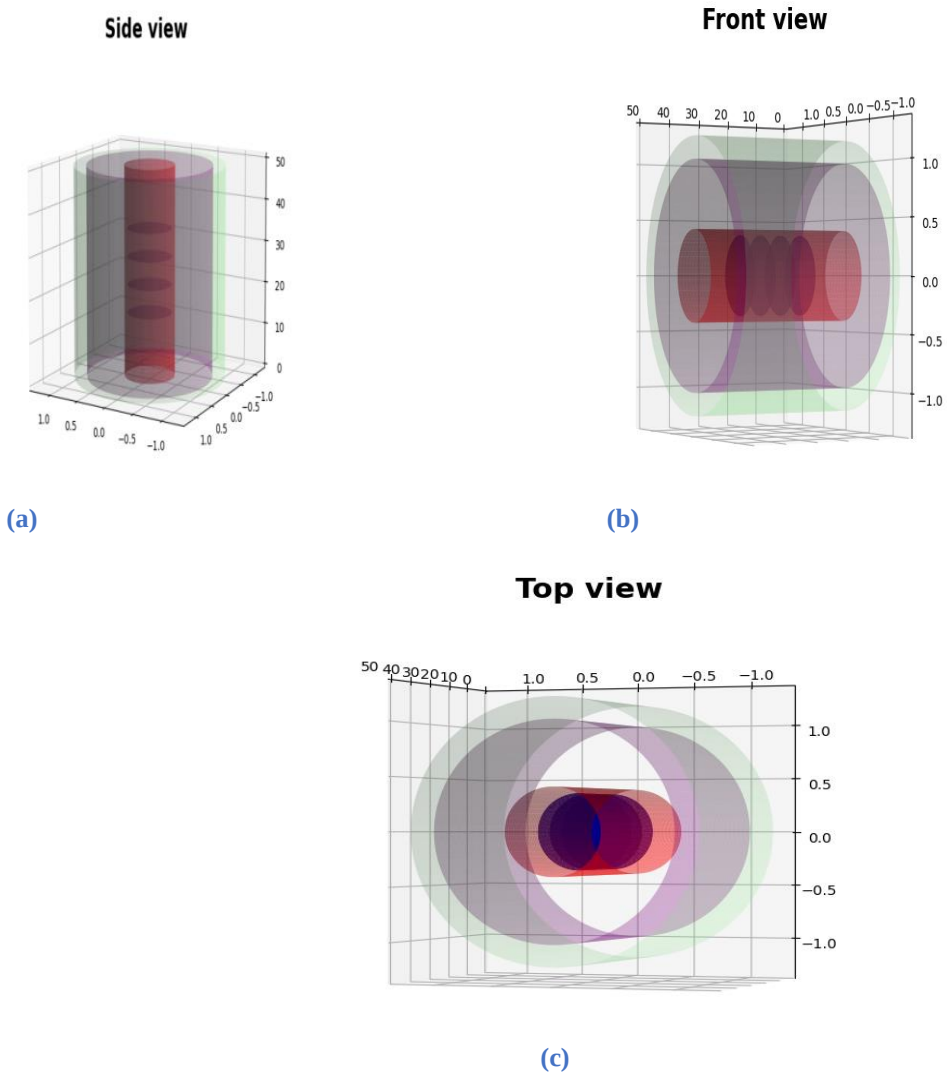

Figure 2:3D image of FBG structure (a) side view, (b) Front view and (c) Top view

Power System Technology
ISSN:1000-3673
Received: 06-10-2024 Revised: 15-11-2024 Accepted: 25-02-2025

The optical interrogator will record and reflect a narrow band wavelength as the broadband laser source is introduced into the optical fibre. The simulation utilizes the VPI photonics Design Suite, where light from a 193.1 THz LED source (1.553 µm wavelength) travels by a 1 m SMF featuring a FBG at its center. The transmitted spectrum of the FBG helps identify the frequency with the lowest power component, allowing for the determination of the peak reflected wavelength. This data is then plotted against depth to assess sensitivity, with underwater depth represented as assessment of pressure that can straight gauged using the FBG by eqn (1)

$$D = \frac{P}{\rho g} \tag{1}$$

Where, D implies depth, P implies pressure, ρ implies underwater thickness, g implies gravitational acceleration. A fundamental premise of our research is the constancy of the ambient refractive index. Therefore, the alter in reflected wavelength occur only because of difference in grating time as outcome of given pressure as expressed in equation (2)

$$\Delta\Lambda = \frac{\Delta P \mu (1-\rho_e)}{Y} \tag{2}$$

here, $\Delta\Lambda$ implies modify in grating time, ΔP implies variation in pressure, μ ratio of Poisson, ρ_e implies photo-elastic coefficient, Y implies Young's modulus. The properties of the coating materials, like ratio of Poisson, photo-elastic coefficient, Young's modulus, significantly influence sensitivity. Consequently, variations in the coating can lead to notable shifts in the reflected wavelength as a depth function is exhibits in equation (3).

$$\Delta\lambda = 2n\Delta\Lambda = \frac{2n\Delta D\mu(1-\rho_e)}{Y\rho_g} \tag{3}$$

Here, ΔD implies alteration in depth. Hence, the sensitive is evaluated as shift in wavelength per unit depth in equation (4)

$$S = \frac{\Delta\lambda}{\Delta D} = \frac{2n\Delta D\mu(1-\rho_e)}{Y\rho_g} \tag{4}$$

here, S implies sensitivity. In the simulation schematic, the refractive index is set at 1.451, seawater density at 1029 kg/m³, as well as gravitational acceleration at 9.807 m/s². Using these parameters, we will examine the sensitivity achieved with various coating resources in the next part, considering 5 options: Polymer (PMMA), Titanium Oxide (TiO2), Boron Nitride (BN), Magnesium Oxide (MgO), Polytetrafluoroethylene. A materials-based parameters of every of these is tabularized in Table 1.

Power System Technology
ISSN:1000-3673
Received: 06-10-2024 Revised: 15-11-2024 Accepted: 25-02-2025

3.2 Ocean depth sensor dependent Ultra-Weak Fibre Bragg Gratings

The UWFBG [21] is proposed for under water applications. The UWFB Gtechnique enhances the capacity of Bragg gratings in fibre-optic cables by reducing their refractive index. This allows for the integration of thousands of UWFBGs within a single fibre core, each capable of measuring strain or temperature. These UWFBGs can be localized by employing time-division multiplexing (TDM), since the incident light's reflection duration changes at different points. Consequently, multiple UWFBGs with identical refractive indices and wavelengths can be multiplexed within the same fibre core, forming a uniform array. The reflection times enable sensor localization, while wavelength shifts provide data on strain or temperature variations is given in equation (5).

Table 1: Material-based parameter

Material	Poisson's ratio ρ_e	Photo elastic coefficient Y	Young's modulus (GPa)
PMMA	0.17	0.139B	70
TiO2	0.45	-	12.74
BN	0.34	-	69
MgO	0.25	-	100
PTFE	0.42	0.0785B	0.5

$$t = \frac{2n_{eff}\, d}{c} \tag{5}$$

here, c implies light velocity in fibre-optic; d signifies UWFBGs interval distant; t implies time interval among receiving 2 UWFBGs wavelengths in fibre. Finally, the Bragg grating's refractive index R is reduced for increase the Bragg grating's capability in the fibre-optic cable.

4. Result and Discussion

This section presents the experimental results of the SEACM-UWFBG-DSUA method, implemented on a computer running Python 3.8 with TensorFlow 2.4, equipped with 64GB

Power System Technology
ISSN:1000-3673
Received: 06-10-2024 Revised: 15-11-2024 Accepted: 25-02-2025

RAM and an Intel Xeon W-2155 CPU at 3.30 GHz. The method's performance is evaluated across various metrics, with the number of iterations reflecting the batches needed to complete one epoch. Using a uniform ocean profile at a depth of 1500 m, overall sensitivity is assessed by varying the depth and measuring wavelength changes. Observations are made at three stationary sites within epipelagic, mesopelagic, bathypelagic zones (sunlight, twilight, midnight) to analyze the transmitted spectra and frequency shifts.

Figure 3 illustrates the analysis of reflected wavelength over the depth of different coating materials. This analysis compares the sensitivity values derived from applying different coatings to the FBG. Notably, PTFE exhibits superior sensitivity compared to metals, as illustrated in the inset.

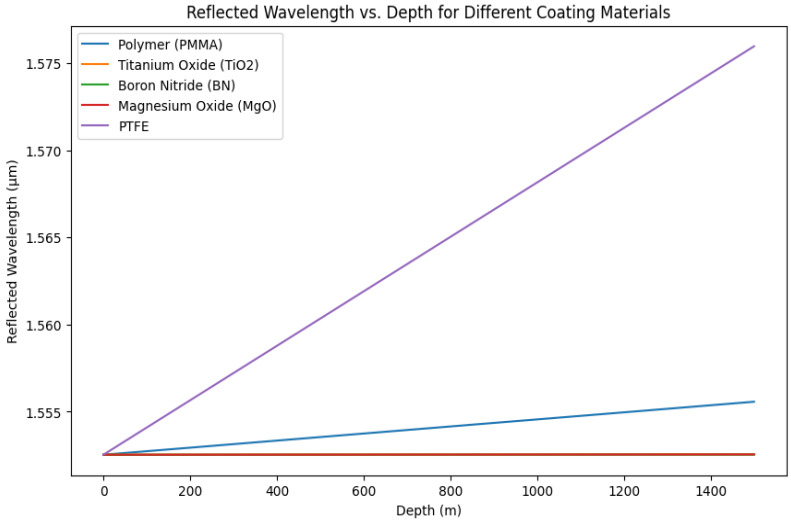

Figure 3: Analysis of reflected wavelength vs. depth of different coating materials

Despite a slight nonlinearity in the 60-180 m range, the sensitivity for PTFE is estimated at 11.8 pm/m. Additionally, the sensitive for other materials, including PMMA, titanium oxide (TiO2), boron nitride (BN), and magnesium oxide (MgO), also evaluated the $0.067 pm/m, 0.967 pm/m, 0.133 pm/m$ *and* $0.067 pm/m$ correspondingly. The sensitive of PMMA as well as MgO are same, as a less value of Young's modulus and a high ratio of Poisson facilitates indium to attain the maximum sensitive amongst the metals. Figure 4 illustrates the transmission spectra of depth 150m. The spectral dips occur at differences of 0.21 THz, 0.89 THz, 1.78 terahertz at referenced point of 193.1 terahertz, corresponding to changes of 0.11%, 0.46%, 0.92%, that are 69, 230, 418 times greater than those of standard TiO2 FBG. Therefore, PTFE emerges as the best coating material among the options evaluated, provided the signal analyzer has adequate bandwidth; otherwise, BN is the next best choice. Figure.5, the output acquired 600 m deep is introduced. The outcome is anticipated similar to

Power System Technology
ISSN:1000-3673
Received: 06-10-2024 Revised: 15-11-2024 Accepted: 25-02-2025

that of Fig. 2, with the frequency shift of a BN-coated FBG far greater than that of other materials. The difference among PMMA as well as MgO is more obvious. The magnitude of shift because of indium, though, decreases to 10.5 times that due to TiO2.

Figure 6 illustrates the transmission spectra of depth 150m. As the depth raises to 1200 m ,the BN-coated FBG witnesses rather a important frequency shift, of 82.1875 GHz. In difference, the deviation in the reflected frequency of TiO2 is a mere 4.375 GHz, a value almost 18.8 times fewer pronounced than that attained from an BN coating.

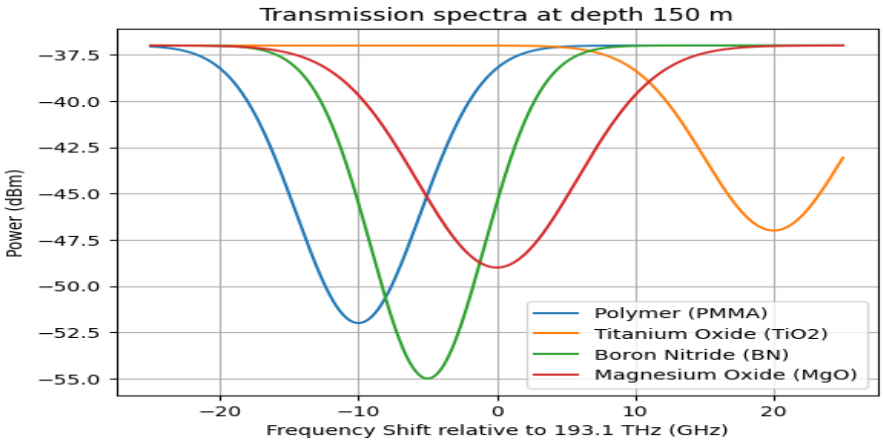

Figure 4: Transmission spectra at depth = 150 m

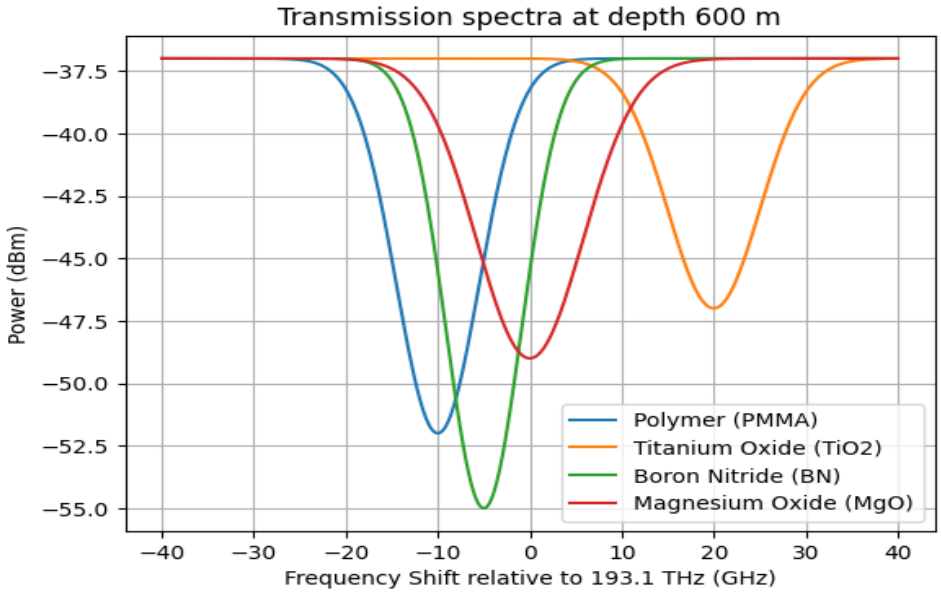

Figure 5: Transmission spectra at depth = 600 m

Power System Technology
ISSN:1000-3673
Received: 06-10-2024 Revised: 15-11-2024 Accepted: 25-02-2025

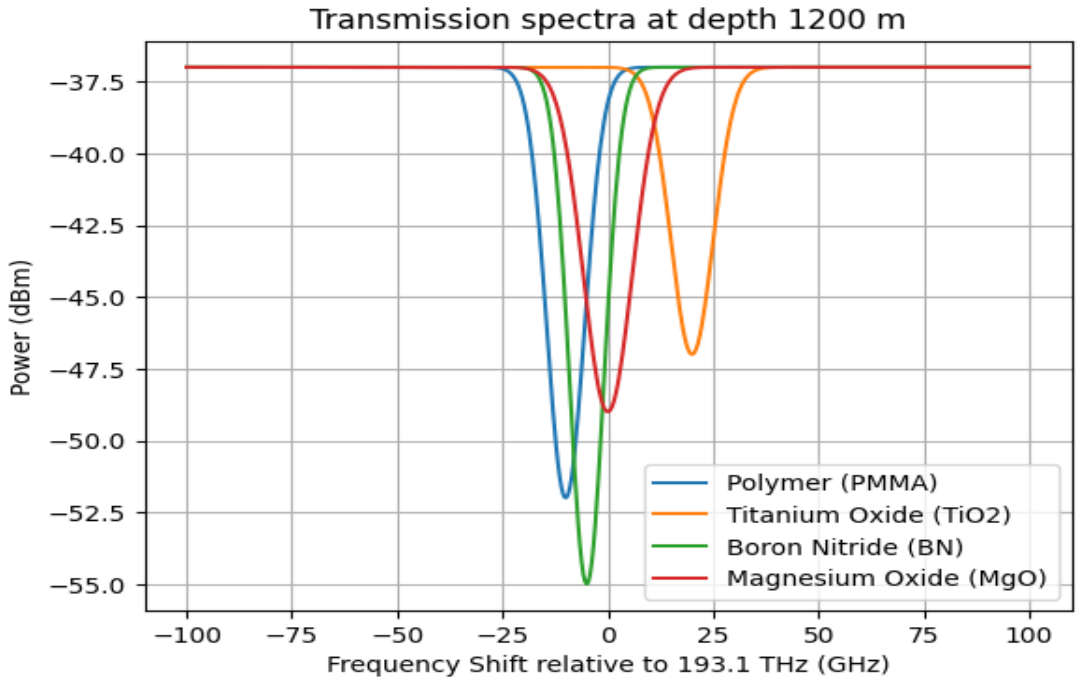

Figure 6: Transmission spectra at depth = 1200 m

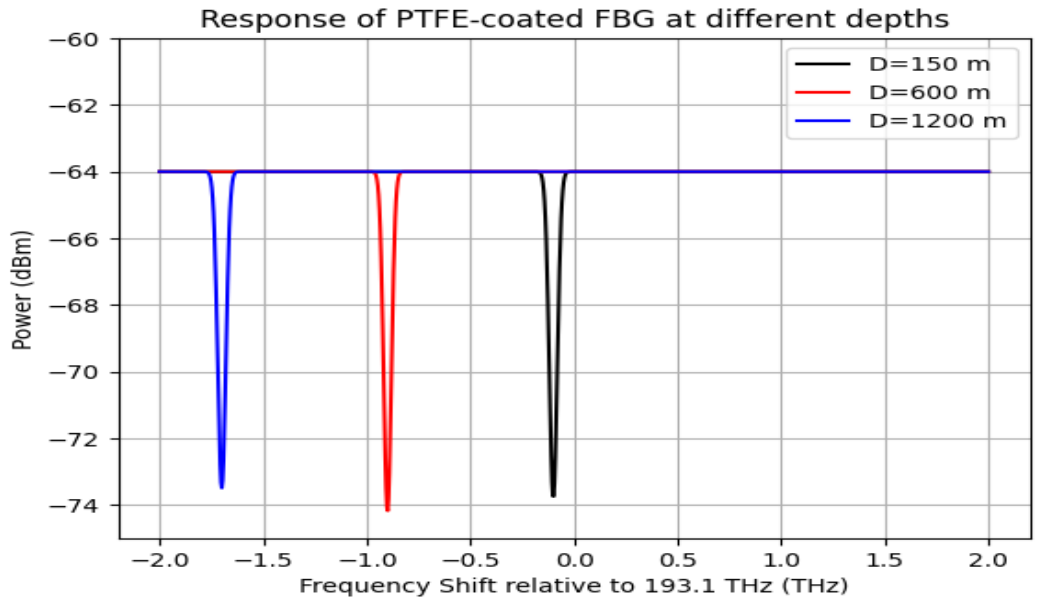

Figure 7: Response of Polytetrafluoroethylene-coated Fibre Bragg Grating at diverse depths

Polytetrafluoroethylene-coated Fibre Bragg Grating at depths of 1200 m, 150 m, 600 m, as illustrates in Figure 7. It's clear that polytetrafluoroethylene has significantly greater sensitivity

Power System Technology
ISSN:1000-3673
Received: 06-10-2024 Revised: 15-11-2024 Accepted: 25-02-2025

than metals, which are examined in more detail in the inset.While there is a small nonlinearity in the $60-180m$ area of the Polytetrafluoroethylene graph, the sensitivity can be approximated as $11.8pm/m$. On the other hand, the corresponding sensitivity of SiO2, In, Al,Znar $0.067pm/m, 0.967pm/m, 0.133pm/m$ *and* $0.067pm/m$ correspondingly. The sensitivity of SiO2as well as Znare same, as a less Young's modulus value with a high ratio of Poisson facilitates indium to attain the maximum sensitive amongst the metals.

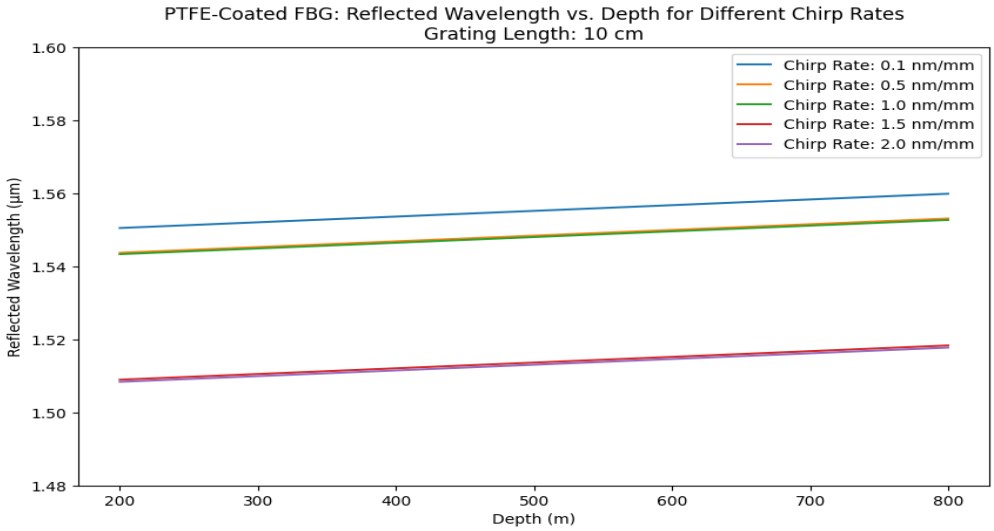

Figure 8: Chirped gratings of length 10 cm

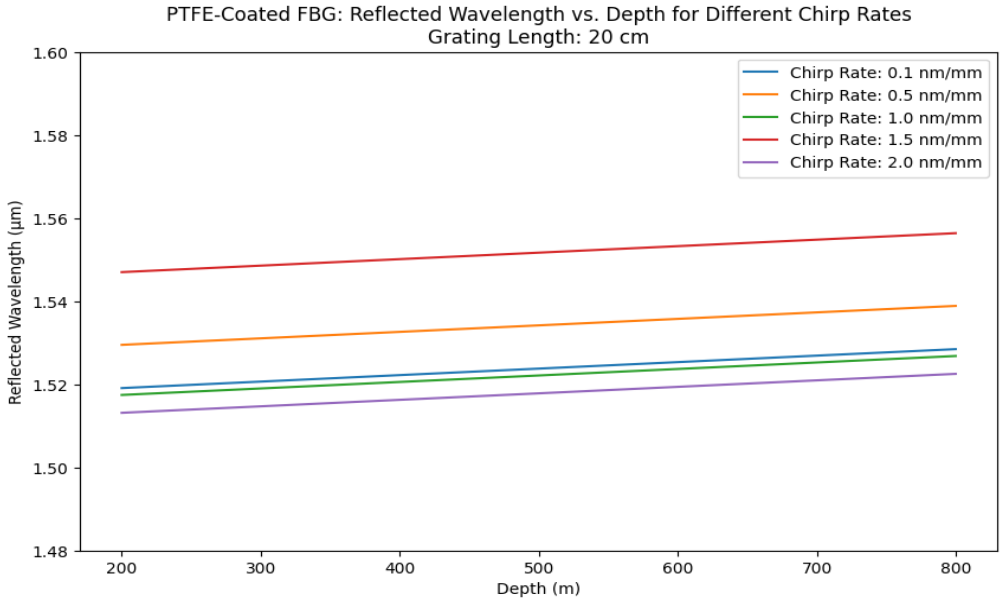

Figure 9: Chirped gratings of length 20 cm

Power System Technology
ISSN:1000-3673
Received: 06-10-2024 Revised: 15-11-2024 Accepted: 25-02-2025

Figure 8 shows chirped gratings with a length of 10 cm including a PTFE coating. Sensitivity differences are not noticeable across a extensive range, thus we project on a depth of 600-800 m. The ideal grating chirp ratio is 1.5 nm/mm, rather than the extremes of 0.1 or 2 nm/mm. On raising the length to 20 cm, in Figure 9, other exciting consequences can be experiential. A significant nonlinearity may be observed in the chirp rate = 1.5 graph. It is discovered that the sensitivity of the ideal rate in the earlier case lagged. The high sensitivity is reached at a chirp rate of 1 nm/mm, attainment a equal value of 23.33 pm/m. The primary interference that can be made from these two graphs is that grating length determines the ideal chirp rate.

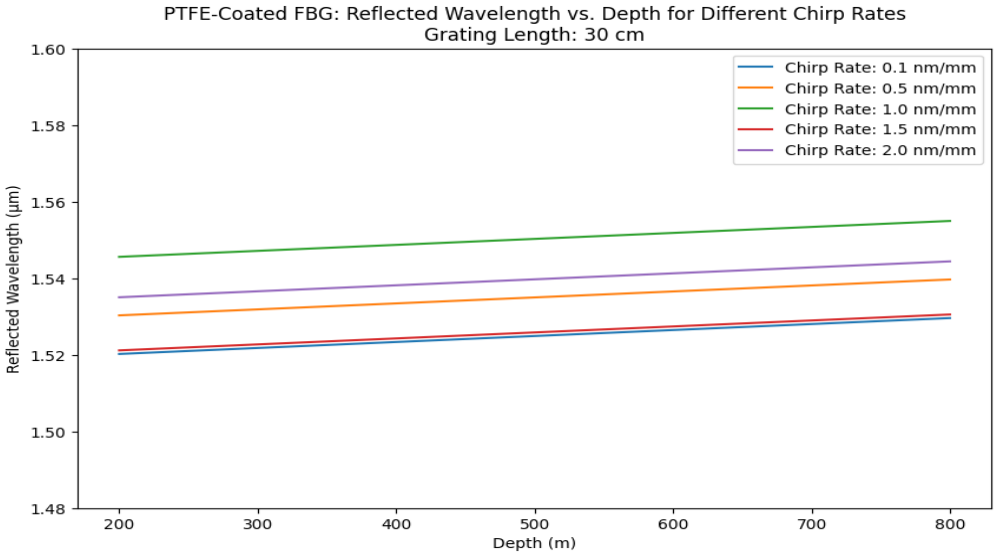

Figure 10: Chirped gratings of length 30 cm

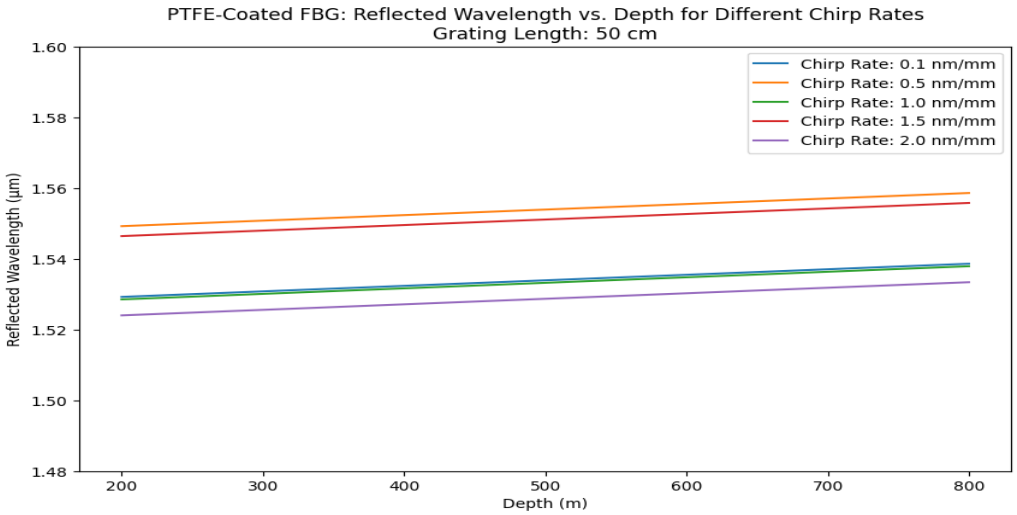

Figure 11: Chirped gratings of length 50 cm

Power System Technology
ISSN:1000-3673
Received: 06-10-2024 Revised: 15-11-2024 Accepted: 25-02-2025

When the length is increased to 50 cm, as shown in Fig. 11, At depths of 675–775 m, we see a nonlinearity at a chirp rate of 2 nm/mm, which leads to a steeper slope, however, 0.1 nm/mm continues to be the most sensitive and consistent chirp rate, although there is no obvious raise in the value of sensitivity.

4.1 Effects of chirping

The chirp rate significantly influences sensitivity, more so than grating length, while duration adversely affects sensitivity at a given chirp rate. Choosing an optimal chirp rate can enhance the sensitivity of the FBG. A pertinent consideration is whether apodization of the grating will further improve performance, specifically by applying a Blackman apodization profile while maintaining a length of 10 cm, according to the eqn (6).

$$A(n) = a_0 - a_1\left(\cos\frac{2\pi n}{N}\right) + a_2\left(\cos\frac{4\pi n}{N}\right) \tag{6}$$

here, $a_0 = 0.42$, $a_1 = 0.5$, $a_2 = 0.08$, chosen in a way that minimize the function's third and fourth side lobes to 0. Weevaluate this alongaeven grating as well as an fibre bragg gratings chirped at $0.1nm/mm$ of similar lengths as well as coating in Figure 12.

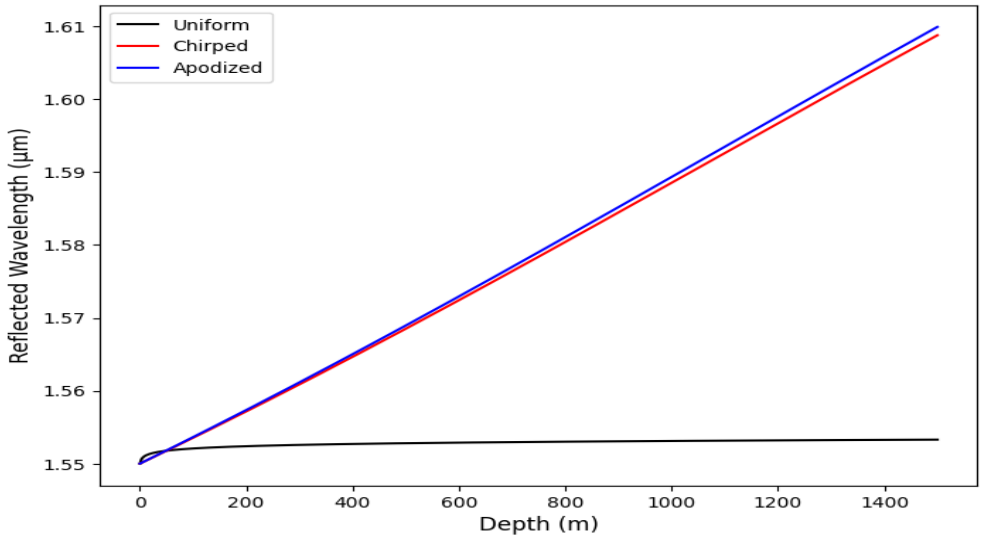

Figure 12: Effects of chirping and apodization on sensitivity

This shows that there is very low variation in the sensitivities of chirped and apodized gratings. Nevertheless, the response of the apodized grating is more linear and stable, leading to sensitivity of $24.54pm/m$. While it is just slightly better than the chirped grating, it is far better than the uniform case. The maximal sensitivity attained is $24.54pm/m$, thus Blackman

Power System Technology
ISSN:1000-3673
Received: 06-10-2024 Revised: 15-11-2024 Accepted: 25-02-2025

apodization on a polytetrafluoroethylene-coated Fibre Bragg Grating. Compared to the consistent silica-coated fiberbragg grating, this represents an enhancement of over 366 times.also a highest deviation of 4.44 terahertz from centre frequency of 193.1 terahertz that is a alter of 2.23%.

4.2 Temperature Compensation

An FBG sensor is affected by changes in both temperature and strain. While we have previously kept the temperature constant, range at 293-298 K at a fixed depth of zero until results in noticeable frequency shifts, illustrates in Figure 13.

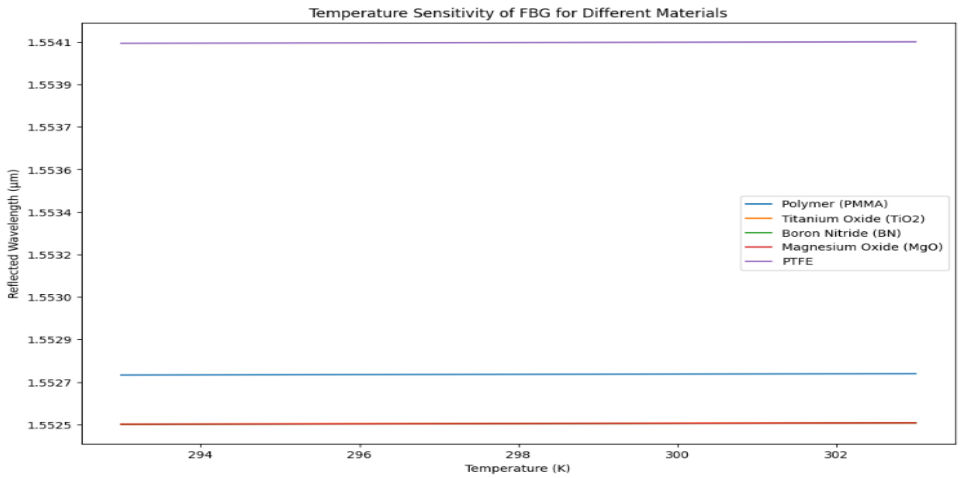

Figure 13: Temperature sensitivities of selected materials

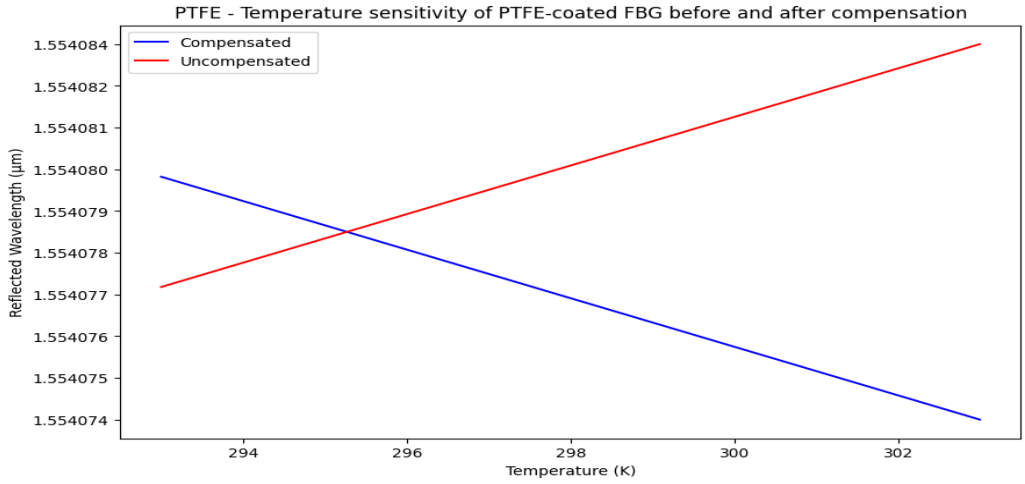

Figure 14: Temperature sensitivity of polytetrafluoroethylene-coated Fiber Bragg Grating before and after compensation

Power System Technology
ISSN:1000-3673
Received: 06-10-2024 Revised: 15-11-2024 Accepted: 25-02-2025

This variation, which is undesirable, correlates with changes in temperature and the Coefficient of Thermal Expansion (CTE). Silica and indium exhibit comparable CTE values, leading to low temperature interference shift of under 3 GHz. In contrast, aluminium and zinc show similar CTEs, leads to the frequency shift close to 25 GHz. Notably, while polytetrafluoroethylene offers the better depth sensitivity, it demonstrates significant temperature cross-sensitivity, with variation of 155 gigahertz at central frequency of 193.1 terahertz. Figure 14 depicts the outcome of temperature compensation operation on 2 similar polytetrafluoroethylene-coated Fibre Bragg Grating for temperature ranging from 293-303 Kelvin. An uncompensated Fibre Bragg Grating exhibits high temperature sensitive, while the compensated arrangement shows no temperature-related changes between 293 and 296 Kelvin, followed by a slight decline at a slope of nanometre/Kelvin. Acorrectreason of mentioneddifference remains unclear but is thought to stem from randomwise attenuation as well asdispersal loss in fibre. The negative sensitivity proposes that this lossismainly concentrated in FBG 1, which appears fewer affected by the similar temperature variations. Additionally, the influence of pressure cross-sensitivity should not be overlooked in this context.

4.3 Performance Analysis

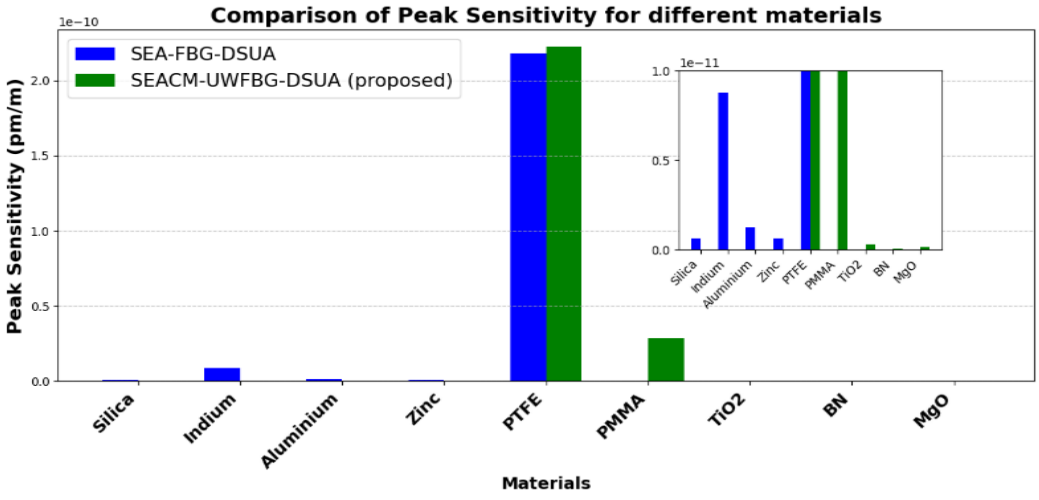

Figure 15: Comparison of peak sensitivity for different materials

Figure 15 illustrates Comparison of peak sensitivity for different materials of proposed SEACM-UWFBG-DSUA.The proposed method shows significantly higher sensitivity across all materials except PTFE, where both methods show zero sensitivity. For example, Silica's sensitivity is around $10^{-8}\ ppmm/m$ with the proposed method, compared to $10^{-10}\ ppmm/m$ with the existing method. This demonstrates the enhanced performance of the SEACM-UWFBG-DSUA method in detecting low concentrations of substances.

Power System Technology
ISSN:1000-3673
Received: 06-10-2024 Revised: 15-11-2024 Accepted: 25-02-2025

Table 2: Comparison table of sensitivity of FBG for all different coating materials

Methods	Materials	Sensitivity (pm/m)
SEA-FBG-DSUA	Silica	0
	Indium	0.1
	Aluminium	0
	Zinc	0
	PTFE	1
SEACM-UWFBG-DSUA (Proposed)	PTFE	2
	PMMA	0.5
	TiO2	0.1
	BN	0
	MgO	0

5. Discussion

In this section, SEACM-UWFBG-DSUA is discussed. This study highlights the significance of coating materials in enhancing the sensitivity of FBG based depth sensors for underwater applications. After evaluating various materials, PTFE emerged as the most effective option, significantly improving sensitivity compared to uncoated sensors. Additionally, the application of modulation techniques like chirp and apodization further optimizes sensor performance, suggesting innovative design possibilities in optical sensing. The research emphasizes addressing the unique challenges posed by maritime environments, which is crucial for developing reliable sensors that can perform simultaneous multi-parameter measurements, such as conductivity, temperature, and depth (CTD). Overall, these findings deepen our understanding of FBG sensor capabilities and provide a foundation for future research and practical applications in oceanography and marine exploration, ultimately leading to more sensitive and robust underwater sensing technologies. This study highlights the significant enhancement in sensitivity of Fibre Bragg Grating (FBG)-based depth sensors achieved through careful selection of coating materials, with PTFE proving to be the most effective. By employing modulation techniques like chirp and apodization, the sensors perform better in challenging underwater conditions. Additionally, the research explores the potential for multi-parameter sensing, including Conductivity-Temperature-Depth (CTD) measurements, addressing the urgent need for reliable underwater sensors while paving the way for advancements in optical sensing technology. The findings offer valuable insights for the

Power System Technology
ISSN:1000-3673
Received: 06-10-2024 Revised: 15-11-2024 Accepted: 25-02-2025

scientific community and have practical implications across various maritime applications, enhancing our capacity to monitor the marine environment. Future work may involve leveraging machine learning algorithms for real-time data interpretation and predictive analytics, as well as investigating the long-term durability and resilience of these sensors to ensure their effectiveness in environmental monitoring, underwater exploration, and resource management.

Acknowledgment
We gratefully thank the Visvesvaraya Technological University, Jnana Sangama, Belagavi for financial support extended to this research work.

References

[1] Braunfelds, J., Haritonovs, E., Senkans, U., Kurbatska, I., Murans, I., Porins, J. and Spolitis, S., 2022. Designing of Fiber Bragg Gratings for Long-Distance Optical Fiber Sensing Networks. Modelling and Simulation in Engineering, 2022(1), p.8331485.

[2] Mahlooji, A. and Azhari, F., 2024. A Fiber-Only Optical Vibration Sensor using Off-CenteredFiber Bragg Gratings. IEEE Sensors Journal.

[3] Li, C., Tong, X., Huang, W., Wang, Y., Zeng, F., Chen, L., Shi, X. and Zeng, C., 2024. Development of a Fast Response, High Accuracy, and Miniaturized Fiber Bragg Grating (FBG) sensor for Fluid Temperature measurement. *IEEE Sensors Journal*.

[4] Pulcinelli, M., D'Antoni, F., Presti, D.L., Schena, E., Carassiti, M., De Tommasi, F. and Merone, M., 2024. Combining Fiber Bragg Grating and Artificial Intelligence Technologies for Supporting Epidural Procedures. IEEE Transactions on Biomedical Engineering.

[5] Xie, X., Song, E., Yuan, Z., Yin, Y., Zhang, Y., Yang, Q., Xu, Z. and Ran, Y., 2024. Fiber-Optic Bragg Grating Sensor for PhotothermallyExaminating Moisture of Meat. Photonic Sensors, 14(3), pp.1-13.

[6] Sahota, J.K., Dhawan, D. and Gupta, N., 2024. Modeling and Analysis of Temperature-Compensated Fiber Bragg Grating Sensor Based on Flexure Hinge Beam and Diaphragm for Low-Pressure Detection. *Arabian Journal for Science and Engineering*, *49*(1), pp.1095-1115.

[7] Luo, W., Wang, Y., Ling, Q., Zhu, X., Wang, X., Gu, Z., Chen, H., Yu, Z., Zhang, Y., Wang, H. and Chen, D., 2024. Simultaneous bending and temperature measurement based on a superimposed fiber grating sensor. Infrared Physics & Technology, p.105371.

[8] Liu, Y., Gong, H., Lu, X., Ni, K. and Zhao, C., 2024. Fiber Bragg grating humidity sensor based on side-polished step-index multimode fiber coated with GO. Optics & Laser Technology, 177, p.111175.

[9] Rjeb, A., Ashry, I., Fakiri, A., Marin, J.M., Banjar, F., Manjalivalapil, S.K., Parvez, A.M., Ng, T.K. and Ooi, B.S., 2024. Monitoring Metal Loss Within Pipelines Using Fiber Bragg Grating Sensors Positioned on Repaired Sleeves. IEEE Access.

[10] Liu, Y., Lin, W., Zhao, F., Zhang, X. and Shao, L.Y., 2024. Dual-Parameter Fiber Sensors for Salinity and Temperature Measurement Based on a Tapered PMF Incorporated With an FBG in Sagnac Loop. *IEEE Photonics Journal*.

Power System Technology
ISSN:1000-3673
Received: 06-10-2024 Revised: 15-11-2024 Accepted: 25-02-2025

[11] Cheung, Y., Jing, Z., Liu, Q., Li, A., Liu, Y., Guo, Y., Zhang, S., Zhou, D. and Peng, W., 2024. Fast-Response Fiber-Optic FPI Temperature Sensing System Based on Modulated Grating Y-Branch Tunable Laser. *Photonic Sensors*, *14*(1), p.240125.

[12] Zheng, Y., Zhang, X., Zhang, J. and Liu, H., 2024. A Polyimide-Coated Fiber Bragg Grating Sensor for Multi-Depth Soil Humidity Measurement. IEEE Sensors Journal.

[13] Zhang, L., Li, C., Dong, H., Liu, X., Sun, T., Grattan, K.T. and Zhao, J., 2023. Fiber Bragg Grating-based sensor system for sensing the shape of flexible needles. *Measurement*, *206*, p.112251.

[14] Liu, F., Wei, S., Li, B., Tan, Y., Guo, X. and Fu, X., 2023. A novel fast response and high precision water temperature sensor based on Fiber Bragg Grating. *Optik*, *289*, p.171257.

[15] Sa'ad, M.S.M., Ahmad, H., Samion, M.Z., Alias, M.A., Zaini, M.K.A., Sing, L.K., Grattan, K.T., Rahman, B.A., Brambilla, G., Harun, S.W. and Ismail, M.F., 2023. A fiber Bragg grating-based inclinometer probe with enhanced sensitivity for a higher slope profiling resolution. Sensors and Actuators A: Physical, 364, p.114804.

[16] Chakravartula, V., Samiappan, D. and Kumar, R., 2020. Sensitivity enhancement analysis due to different coating materials of Fibre Bragg Grating-based depth sensor for underwater applications. Optical and quantum electronics, 52, pp.1-15.

[17] Naumann, C., Carlesi, T., Otto, H., Cierpka, C. and Laboureur, D., 2024. Dynamic characterization of Fiber Bragg Grating temperature sensors. *Experimental Thermal and Fluid Science*, *156*, p.111222.

[18] Haque, M.A., Rahad, R., Faruque, M.O., Mobassir, M.S. and Sagor, R.H., 2024. Numerical analysis of a metal-insulator-metal waveguide-integrated magnetic field sensor operating at sub-wavelength scales. Sensing and Bio-Sensing Research, 43, p.100618.

[19] MACHESO, P.S. and ZEKRITI, M., 2024. Modelling and Analysis of Fiber Bragg Grating Temperature Sensor for Internet of Things Applications (FBG-4-IoT). International Journal of Intelligent Networks.

[20] Liu, X., Yin, B., Li, H., Wang, M., Yan, R., Li, Y., Zong, C. and Wu, S., 2023. Highly sensitive sensor for simultaneous underwater measurement of salinity and temperature based on highly birefringent asymmetric photonic crystal fiber. *Results in Optics*, *11*, p.100406.

[21] Liu, S.P., Shi, B., Gu, K., Zhang, C.C., He, J.H., Wu, J.H. and Wei, G.Q., 2021. Fiber-optic wireless sensor network using ultra-weak fiber Bragg gratings for vertical subsurface deformation monitoring. *Natural Hazards*, *109*, pp.2557-2573.